Catalysis Today 418 (2023) 114123

Contents lists available at ScienceDirect

Catalysis Today

journal homepage: www.elsevier.com/locate/cattod

Minimizing rare earth content of FCC catalysts: Understanding the fundamentals on combined P-La stabilization

Cristina Martínez [a,*], Alejandro Vidal-Moya [a], Bilge Yilmaz [b], CP Kelkar [b], Avelino Corma [a,*]

[a] Instituto de Tecnología Química (UPV-CSIC), Universidad Politècnica de València-Consejo Superior de Investigaciones Científicas, Avda. de los Naranjos s/n, Valencia 46022, Spain
[b] BASF Corporation, 25 Middlesex-Essex Turnpike Iselin, Iselin 08830, United States

ARTICLE INFO

Keywords:
Catalytic cracking
Zeolite USY
Hydrothermal stabilization
Phosphorus
Rare earth

ABSTRACT

Fluidized Catalytic cracking (FCC) is one of the main conversion processes in conventional refineries and employs a multicomponent catalyst with Y zeolite as the main source of activity and selectivity towards value added products. In order to meet the severe requirements of the FCC unit, the hydrothermal stability of this large pore zeolite is traditionally improved by means of controlled hydrothermal treatments that can be combined with acid washing cycles, with rare earth (RE) ion exchange or with a combination of both. Phosphorus has also been described as a hydrothermal stabilization element. Although most of the studies are based on ZSM-5 zeolites, a new Y zeolite containing FCC catalyst, Phinesse™, was developed recently. This catalyst, based on the partial substitution of RE by P allowed obtaining the same activity and the same yields to the main products as its conventional RE stabilized counterpart in the catalytic cracking of a vacuum gas oil (VGO). In this work, we present a systematic study where the hydrothermal stability of P- and La-free USYs with different dealumination degrees is compared with that of the corresponding USYs containing P or La alone or a combination of both stabilizing elements. The samples have been thoroughly characterized and their catalytic performance has been tested in a MAT unit. According to the results obtained, when using RE alone, only high contents (> 3.5 wt% RE) are able to stabilize the catalysts towards steaming under severe conditions (100% steam, 750 ºC). However, lower RE (wt%) can lead to similar hydrothermal stabilization when combined with intermediate phosphorus contents (~1.0 wt%). The results obtained provide the bases for understanding the reasons behind the benefits of this combined P-La stabilization observed for the commercial Phinesse™ catalyst as compared to a high REO catalyst.

1. Introduction

Fluidized Catalytic cracking (FCC) is one of the main conversion processes in conventional refineries [1–3]. Although traditionally directed to the production of liquid fuels, FCC has been adapted in order to deal with changes in environmental regulations and changes in the market, such as the integration of biomass- or other waste-derived feedstocks within the existing petroleum refining infrastructure, or the increasing demand for light olefins [4–7].

FCC employs a multicomponent catalyst, with Y zeolite as the main source of catalytic activity and selectivity since the 1960 s. Inclusion of zeolites in FCC catalysis led to a step increase in the efficiency of utilization of crude oil derived feedstocks in this key conversion process and thus had direct impact on the industrial society. In order to meet the requirements of the FCC unit, the hydrothermal stability of this large pore zeolite needs to be improved. Traditionally this has been done by means of controlled steaming and acid washing cycles, leading to the ultra-stable Y (USY), by ion exchange with rare earths (RE) ions or by a combination of both (REY and RE-USY, respectively).

Hydrothermal treatment leads to framework dealumination, and to the generation of extra-framework aluminum (EFAl) species that exert a stabilization role [8,9]. The presence of these EFAl species has a strong effect on the zeolite's acidity, not only by reducing the number of Brønsted acid sites (BAS) and creating new Lewis acid sites (LAS), [10] but also by the interaction of these non-framework Al^{3+} cations with framework Al (FAl) [11]. The textural properties are also affected, and the creation of mesopores results in an increased accessibility [12,13]. Steaming conditions have, therefore, a direct influence on the

* Corresponding authors.
E-mail addresses: cmsanche@itq.upv.es (C. Martínez), acorma@itq.upv.es (A. Corma).

https://doi.org/10.1016/j.cattod.2023.114123
Received 12 December 2022; Received in revised form 28 February 2023; Accepted 16 March 2023
Available online 20 March 2023

physicochemical properties of the final USYs and will determine their catalytic activity and selectivity [14–18].

RE introduction into the charge compensation sites stabilizes zeolite Y by preventing dealumination and diminishing the acid catalyzed hydrolysis of the Si-O-Al bond. This results in an increase of the BAS density of the working catalysts as compared to USY, but without the generation of mesoporosity [19]. A consequence of the higher hydrothermal stability of RE-containing FCC catalyst is a higher activity and higher yields in fuels. On the other hand, it increases the hydrogen transfer capacity leading to lower octane and lower olefinicity in the LPG fraction [3,19,20].

The RE ion exchange in zeolite, the location of La in the Y zeolite, and the effect of calcination on the location, on the valence of the La ions, and on zeolite dehydroxylation were extensively studied in the 1980′s and early 1990′s [21–29]. In the case of lanthanum cations, they are mainly located as polynuclear hydroxylated clusters within the sodalite cages, although they can also be present in the supercages for high La contents or as monomeric La^{3+} within the double six-ring (D6R) units connecting the sodalite cages [23,30,31]. The latter are, however, less favored in high-silica faujasites [30]. Structural and catalytic –cracking-properties were also studied on LaY and LaUSY and compared to those of HY and HUSY, [22,32] but RE contents were in some cases considerably higher (3–20 wt% La_2O_3) than those used nowadays.

Phosphorus has also been described as a stabilizing element. Although the role of phosphorus has been thoroughly studied for hydrothermal stabilization of ZSM-5, [33] little can be found on the mechanism for P stabilization of large pore USY zeolite. Still, early work by Corma et al. [34,35] evidenced the interaction of H_3PO_4 with EFAL in ultrastable Y zeolites (USY) leading to the formation of different type of aluminum phosphates and the consequences that this had on the acidic properties of the USY zeolites. Regarding the catalytic behavior, P stabilization resulted in an increased activity and reduced selectivity to dry gas and coke [36]. Other examples of the use of phosphorus as a possible substitute of REO (total or partial) in FCC catalysts can also be found in the patent literature [37–41].

In response to the huge increase of lanthanum prices in 2011, and after the drastic reduction of export quotas by China as the main REO provider worldwide, BASF developed a new FCC catalysts combining phosphorus-stabilization on Y zeolite with reduced REO contents [42]. This catalyst, Phinesse™, based on the Distributed Matrix Structure (DMS) technology, [43] was designed to give the same yield structure and activity as the incumbent catalyst in vacuum gas oil (VGO) feed applications, but with 50% less RE. After a successful scale up, performance of this new catalyst technology was first demonstrated in 2012–2013 as part of an industrial field trial at the Shell Sarnia refinery [42].

Here, we present a systematic study where P- and La-free USYs with different dealumination degrees are compared with the corresponding USYs containing P or La alone or their combination. Correlating their physicochemical properties with their catalytic behavior provides the clues for understanding the benefits of the combined P-La stabilization.

2. Experimental

2.1. Catalyst preparation

Three ultrastable Y (USY) zeolites were prepared by pre-stabilization at different temperatures as follows. In a first step, a partially ammonium exchanged NaY zeolite was prepared starting from commercial NaY zeolite CBV100 (Zeolyst Int.) by adding 100 g of NaY to 1000 g of a 2.5 M solution of NH_4Cl (Sigma, ≥99.5%), and keeping it under vigorous stirring for one hour at 80 ºC. The solid was separated by filtration and washed until total removal of chlorides. Then it was dried at 100 ºC overnight and the ion exchange was repeated. This NH_4NaY sample (2.2 wt% Na_2O, Na/Al=0.18 mol/mol) was then calcined in a 100% steam atmosphere at 500, 600 and 700 ºC, forcing in this way the remaining sodium cations to move out of the sodalite cages. Then the Na was removed by further ion exchange with NH_4Cl, as described above, to obtain the fully protonic form of the zeolites, and the samples were calcined at 500 ºC for 3 h. The NH_4Cl exchange and calcination steps were done twice. The pre-stabilized USYs were named as USY500, USY600 and USY700.

High REO USY samples were prepared by ion exchange with a 0.1 M $LaCl_3{\cdot}7H_2O$ (Sigma Aldrich, 99.9%) solution, at 80 ºC for 2 h under vigorous stirring. After separating the solid by filtration it was thoroughly washed, dried at 100 ºC overnight, and calcined at 500 ºC for 3 h. These two steps (REO exchange + calcination) were done twice.

USY600 was ion exchanged with $LaCl_3{\cdot}7H_2O$ (Sigma Aldrich, 99.9%) solutions of different concentrations, at 80 ºC for 2 h under vigorous stirring, in order to obtain samples with increasing La_2O_3 contents. Thus, keeping a solution to zeolite ratio of 10 (wt/wt), the concentration of $LaCl_3$ was calculated for a target La_2O_3 wt% of 0.5, 1.0, 2.0 and 4.0 wt%, in case of complete ion exchange. After separating the solid by filtration, it was thoroughly washed, dried at 100 ºC overnight, and calcined at 500 ºC for 3 h. These two steps (REO exchange + calcination) were done twice for the high-La samples (4 wt% La_2O_3).

P-stabilized USY600 samples with different P contents, in the range of 0.5–3.0 wt%, were prepared by wet impregnation by suspending the zeolite in an aqueous H_3PO_4 (Sigma Aldrich, 85%) solution of the corresponding concentration maintaining a liquid-to-solid ratio of 10 (wt/wt). The suspension was slowly evaporated (during 1 h) in a rotary vacuum evaporator at 80 ºC until dry. Then the samples were dried at 100 ºC overnight and calcined at 500 ºC for 1 h. Part of these samples was ion exchanged with La in a second step: therefore, the P/USY was added to a 0.03 M solution of $LaCl_3{\cdot}7H_2O$ (Sigma Aldrich, 99.9%), stirred vigorously for 2 h at 80 ºC, separated by filtration, washed and dried at 100 ºC overnight. The resulting solid was calcined for 3 h at 500 ºC. Phosphorus containing USYs using ammonium dihydrogen phosphate (Sigma Aldrich, 99.9%, MAP) and ammonium hydrogen phosphate (Sigma Aldrich, 99.9%, DAP) as phosphorus source were prepared following the same impregnation procedure as the H_3PO_4 treated samples varying only the P containing compound.

In order to study the hydrothermal stability of the different samples, they were calcined in a muffle oven for 5 h at 750 ºC in a 100% steam atmosphere (ST).

2.2. Catalyst characterization

Specific surface area of the catalysts was determined in a Micromeritics ASAP 2000 equipment by means of nitrogen adsorption at 77 K and applying the BET-method. Prior to the adsorption measurements, the samples were degassed at 450 ºC for 24 h. Their chemical composition was determined by means of a 715-ES inductively coupled plasma (ICP) Optical Emission spectrometer after dissolution of the solids in a HNO_3/HF solution. The crystalline structure of the solids was confirmed by powder X-ray diffraction (XRD) using a Philips X′Pert diffractometer equipped with a graphite monochromator, operating at 40 kV and 45 mA and using nickel-filtered Cu Kα radiation (λ = 0.1542). XRD was also used to determine the unit cell (UC) constant (a_0) of the USY zeolites following ASTM procedure D-3942–80, and the number of framework aluminums (FAL) was calculated according to the unit cell constant by means of the Breck and Flanigen correlation (Eq. 1) for bulk Si/Al< 3, or with the Fichtner-Schmittler equation for zeolites with bulk Si/Al> 3 (Eq. 2):

$$N_{Al} = (a_0\text{-}24{\cdot}191)/0{\cdot}00868 \quad (1)$$

$$N_{Al} = (a_0\text{-}24{\cdot}233)/0{\cdot}00889 \quad (2)$$

The relative concentration of acidic sites in the different samples was obtained by FT-IR spectroscopy using pyridine as the probe molecule. Pyridine adsorption/desorption experiments were carried out on self-supported wafers (10 $mg{\cdot}cm^{-1}$) activated at 400 ºC and 10^2 Pa for 2

Table 1
Physico-chemical properties of the aged Phinesse™ and NaphthaMax catalysts.

	Phinesse	NaphthaMax
REO, wt%	1.11	1.73
P_2O_5, wt%	1.43	—
Al_2O_3, wt%	39.92	40.84
Total Surface Area (TSA), m^2/g	154	148
Matrix Surface Area (MSA), m^2/g[a]	44	44
Unit Cell Size (UCS), Å	24.29	24.32
RE on zeolite ratio[b]	7.32	11.88

[a] MSA determined as the TSA minus the micropore surface area
[b] RE on zeolite ratio determined as total RE loading referred to zeolite content in the catalyst

Table 2
CRU tests: activity at C/O 11.5 and selectivities at constant gasoline conversion of 78%.

	Phinesse™	NaphthaMax
2^{nd} order Activity @ C/O= 11.5	3.6	3.9
Gasoline Conversion @ C/O= 11.5, %	78.0	79.5
Bottoms Conversion @ C/O= 11.5, %	93.1	94.1
H_2, wt%	0.1	0.1
Total C_{2-}, wt%	2.2	2.2
LPG, wt%	16.8	16.4
Gasoline, wt%	51.5	52.1
LCO, wt%	15.0	15.2
Bottoms, wt%	6.9	6.8
Coke, wt%	7.1	7.0
$C_3^=$/Total C_3s, wt/wt	0.8	0.9
$iC_4^=$/iC_4, wt/wt	0.7	0.7
Total $C_4^=$s/Total C_4s, wt/wt	0.6	0.7

h. After sample activation, pyridine vapor ($6.5.10^2$ Pa) was admitted into the vacuum IR cell and adsorbed onto the zeolite at room temperature. Desorption was performed under vacuum over three consecutive 1 h periods of heating at 250, 350, and 400 ºC, each followed by an IR measurement at room temperature. All of the spectra were scaled according to the sample weight.

Solid-state NMR spectra were recorded under magic angle spinning (MAS) at room temperature in a Bruker AVANCEIII-HD spectrometer, ^{27}Al NMR spectra were recorded at 104.2 MHz with a spinning rate of 20 kHz and a 9º pulse length of 0.5 μs with a 0.5 s repetition time. ^{27}Al chemical shifts were reported relative to $[Al^{3+}(H_2O)_6]$. ^{31}P NMR spectra were recorded at 161.9 MHz with a spinning rate of 20 kHz and a 67.5º pulse length of 4.9 μs with 15 s repetition time. The chemical shifts were reported relative to 85% H_3PO_4.

2.3. Catalytic tests

The cracking of NaphthaMax and PhinesseTM equilibrium catalysts was performed in a circulating riser unit (CRU). CRU testing was carried out by loading about 2.5 kg of the Equilibrium catalyst, as fluidizable microspheres, in the unit. The unit pressure is controlled at ~ 2 bar, riser outlet temperature is controlled at 530 °C and riser inlet temperature is generally around 600 °C, although it may vary slightly depending upon catalyst circulation rate. During operation, feed rate is held constant and catalyst-to-oil ratio is varied by varying the circulation rate. Feed preheat temperature is varied between 100 °C and 300 °C. Pre-heated feed is atomized with a mixture of steam and nitrogen and fed through an injector. The regenerator dense bed temperature is typically held constant around 750 °C, and increases slightly as circulation rate slows down. Excess O_2 at the outlet of regenerator is maintained to ensure full combustion of coke. In a typical run, the catalyst-to-oil ratio was varied between 6 and 12. After stripping, the gaseous products were sent to an online Gas Chromatograph equipped with a TCD and an FID detector. The catalyst was continuously regenerated and the effluent gases were analyzed for all gases including H_2O. The liquid syncrude was separately analyzed by ASTM-2887-D procedure and cuts were made at 150.8 ºC for light gasoline, 216.3 ºC for heavy gasoline and 359 ºC for LCO. A combination of all the yields were used to generate a full mass balance. Most runs had a mass balance between 97 and 99 wt%. Gasoline conversion is defined as the sum of gases, gasoline and coke yields. Bottoms conversion is defined as the sum of gases, gasoline, LCO and coke yields.

Catalysts prepared in-house were tested in a Microactivity Test (MAT) unit at 520 ºC and 15 s time. The MAT unit is fully automated and can be operated in a continuous way up to eight cycles, i.e. stripping-reaction-regeneration, without operator intervention. The reaction zone and product recovery system have been designed in accordance with ASTM D-3907. The reactions were carried out at 520 ºC and with a catalyst time on stream (TOS) of 15 s. In order to vary the conversion, the catalyst-to-oil ratio was varied in a range of 2–6 g/g keeping the amount of catalyst constant (3 g), and changing the amount of oil fed. The catalyst bed contained 0.3 g of the USY zeolite pelletized, crushed and sieved to a particle size in the range of 0.4–0.6 mm, diluted with 2.7 g of silica (0.2–0.4 mm). Before each experiment, the system was purged with a 30 cm3/min N2 flow for 30 min at the reaction temperature. After reaction, stripping of the catalyst was carried out for 15 min using a N2 flow of 30 cm^3/min. During the reaction and stripping steps, the liquid products were collected in the corresponding glass receivers located at the exit of the reactor, kept at 10 ºC by means of a computer-controlled bath. Meanwhile the gaseous products were collected in a gas burette by water displacement. After stripping, the catalyst was regenerated at 540 ºC for 3 h, in a 100 cm^3/min stream of air.

The gases were analyzed using a Varian 3600-GC equipped with three detectors. A thermal conductivity detector (TCD) was used for analysis of H_2 and N_2, which were separated in a 15 m molecular sieve column, and a flame ionization detector (FID) for C1 to C6 hydrocarbons separated in a 30 m Plot/Al_2O_3 column.

Simulated distillation of the liquids was carried out with a Varian 3800-GC following the ASTM-2887-D procedure. Cuts were made at 150.8 ºC for light gasoline, 216.3 ºC for heavy gasoline and 359 ºC for LCO. Gasoline and bottoms conversion are defined as in the case of the CRU tests.

The properties of the vacuum gasoils (VGOs) used in the CRU and in the MAT experiments are given in Tables S1 and S2, respectively.

3. Results and discussion

3.1. Phinesse™ vs NaphthaMax

The catalytic behavior of two commercial FCC catalysts, Phinesse™ and NaphthaMax, was evaluated in a Circulating Riser Unit (CRU) as described in the experimental section. As reported in earlier literature, Phinesse™ is a BASF catalyst that uses phosphorus as hydrothermal stabilization element, and that has been designed to give the same activity and yields as BASF's NaphthaMax III® but with 50% less RE. When comparing the physicochemical properties of the two aged catalysts enclosed in Table 1, the hydrothermal stability of Phinesse™ is, indeed, very close to that of NaphthaMax, despite the reduction in REO from 1.73 to 1.11 wt%. The total surface area (TSA) of Phinesse™ is slightly higher than that of NapthaMax and, considering that the matrix contributes in both cases with 44 m^2/g, the higher TSA of the P-containing catalyst is due to a higher zeolite surface area (ZSA), which provides the evidence of a comparable, if not better, structural preservation. Although the UC size of NaphthaMax, slightly higher as compared to that of Phinesse™, suggests a lower framework dealumination degree of the former, this higher UC size can also be due to an increase in the T-O-T angles of the zeolite structure caused by the presence of cationic RE species in ion-exchange positions [3,29,31]. Thus, the characterization results confirm that the introduction of P is able to compensate the decrease in REO in the Phinesse™ catalyst regarding hydrothermal stability.

Table 3
Physico-chemical properties of different USY samples and La-USYs.

Sample	UCS (Å ± 0.03)	Si/Al_{TOT} (ICP)	Si/Al_{FAL} (UCS)	$\%La_2O_3$	BET (m^2/g)	V_{micro} (cm^3/g)	V_{meso} (cm^3/g)	BAS[a] (a.u.)	LAS[a] (a.u.)
USY500	24.51	2.5	4	—	688	0.32	0.04	402	263
USY600	24.49	2.5	5	—	663	0.29	0.09	411	273
USY700	24.38	2.5	8	—	547	0.18	0.15	199	257
USY500-ST	24.34	2.5	10	—	585	0.26	0.09	101	168
USY600-ST	24.35	2.5	10	—	589	0.25	0.12	123	186
USY700-ST	24.26	2.5	23	—	466	0.14	0.18	42	76
LaUSY500-ST	24.49	2.5	5	3.6	596	0.27	0.07	113	77
LaUSY600-ST	24.43	3.1	8	4.7	578	0.23	0.12	99	85
LaUSY700-ST	24.33	2.8	11	3.3	448	0.14	0.18	52	33

[a] BAS and LAS determined by FT-IR combined with pydirine adsorption and desorption at 250 ºC.

In good agreement with previous results [42] and with the physicochemical properties discussed above, the decrease in the REO content does not penalize the activity of Phinesse™ (see Table 2), and the gasoline and bottoms conversions obtained with the combined P-La stabilization is comparable to that of the reference NaphthaMax catalyst (see Table 2). Moreover, no problems derived from the use of the phosphorus were experienced, related to phosphorus loss, neither in the CRU nor in previous commercial trials [42].

3.2. Step-by-step preparation of P-La stabilized USYs

The results presented in the former section have shown that partial substitution of REO by phosphorus led to a catalyst with a very similar activity and selectivity than higher REO-based catalysts. This represents an important advancement from the FCC catalyst manufacturing perspective because of the reduced dependency for this raw material, improving supply security as it has a history of dramatic fluctuations in recent history, but also from an environmental and sustainability point of view, as lanthanum is one of the so called critical raw materials (CRM) [44]. The following sections enclose a thorough and rationalized study aiming to understand the stabilization role of P and La alone as compared to the stabilization offered by the P-La combination.

3.2.1. Reference catalysts: USYs vs high REO-USYs

The physicochemical properties of the starting USY zeolite (dealumination degree, textural and acidic properties) will have a direct influence on the amount, the type and the location of the P and/or La species formed when they are incorporated as hydrothermal stabilization elements. In order to study this effect, three different USY zeolites were prepared by pre-stabilizing a partially exchanged NH_4NaY zeolite at 500, 600 and 700 ºC in the presence of 100% steam, followed by ammonium exchange and calcination in order to obtain the fully acid form of the zeolites (samples USY500, USY600 and USY700). The framework dealumination degree and the structural degradation increase progressively by increasing the severity of the pre-stabilization step, as evidenced by the reduction of the UC size, on the one hand, and of the micropore volume on the other (see Table 3). Moreover, as expected, mesoporosity is generated when increasing the temperature of this first steam treatment [12].

The three USY's have been further stabilized by means of a longer hydrothermal treatment (5 h), in a 100% steam atmosphere at 750 ºC (ST). Again, the higher the pre-stabilization temperature, the larger the framework dealumination degree, and the lower the micropore volume of the final sample (see Table 3). Although differences are small when comparing the USY500 and USY600 based samples, the pretreatment at 700 ºC results in an important dealumination of the final zeolites and a substantial structure degradation.

Regarding the acidity of parent USY500, − 600 and − 700 samples (see Table 3 and Table S3), the sample pretreated at the intermediate temperature, USY600, presents the highest total Brønsted acid site (BAS) density, and also the highest proportion of these sites able to retain pyridine at a desorption temperature of 400ºC. In good agreement with the physico-chemical properties presented before, sample CBV700 is considerably less acidic than the other two zeolites. Regarding the amount of Lewis acid sites (LAS), related to the presence of highly dispersed cationic EFAl species, [17] the differences when comparing samples USY500 and USY600 are small, as could be expected from the similar dealumination degree indicated by their UC size values. However, sample USY700 presents a considerably lower number of LAS, despite its higher framework dealumination. Probably part of the EFAl generated in USY700 is polymerized in a larger degree, resulting in a decrease in the number of Lewis acid sites [12,45].

Steaming of the three USY samples at 750 ºC results in an important reduction of the number of total and strong BAS (see Table 3 and Table S3), especially for the USY700 based samples, which also present the lowest amount of LAS. Pre-stabilization at 600 ºC results in the final USY sample, USY600-ST, with the highest BAS density.

Thus, in the absence of P or REO, low pre-stabilization temperatures (500–600 ºC) generate well dispersed EFAl species that preserve the zeolite structure when further steamed at 750 ºC, [17] maintaining UC size values around 24.35 Å and micropore volumes close to 0.250 cm^3/g. However, when pre-treated at higher temperature, e.g. 700 ºC, the EFAl species generated present a larger degree of polymerization, and do not exert this stabilization role. It is important to remark that the dealumination degree and the type of Al species formed during this pre-stabilization step may play a role in the way P and La will be incorporated into the zeolite.

The catalytic behavior of these three USY samples, steamed at 750 ºC, has been evaluated in a MAT unit at 520 ºC and 15 s TOS as described in the Experimental section. Their activity decreases when increasing the severity of the pre-treatment step (see Table S4) and, whereas the differences between USY500 and USY600 are small, the activity loss is significant when the pre-stabilization temperature is increased to 700 ºC. The selectivities, compared at a constant bottoms conversion of 85%, follow the expected trends. The higher the dealumination degree of the zeolite, the higher the selectivity to H_2 and dry gas (C_1 +C_2), and the higher the olefinicity of the LPG fraction (C_3 +C_4) due to a lower BAS density and a lower hydrogen transfer capacity. Regarding coke, USY600 presents the lowest selectivity.

In a second set of samples, the pre-stabilized USY500, USY600 and USY700 zeolites have been converted to high La-content USYs before the final hydrothermal treatment at 750 ºC in order to cover the two extremes, La free and high REO catalysts. Thus, the parent USYs have been ion exchanged in order to obtain La_2O_3 loadings in the range of 3–4 wt% (see Table 3). The lower La uptake after the pretreatment at 700 ºC may be due to a reduced exchange capacity of this sample, as a consequence of its higher dealumination degree [30]. The UC sizes of the La-containing USYs are higher than those of the corresponding La-free samples when steamed at the same temperature (see values enclosed in Table 3), and this could be related to a lower framework dealumination for the La-USYs, but also to the increased T-O-T bonds due to the presence of the RE [30,31]. In fact, the micropore volume of the samples is not affected by the presence or absence of lanthanum, indicating comparable degrees of structure preservation in both cases.

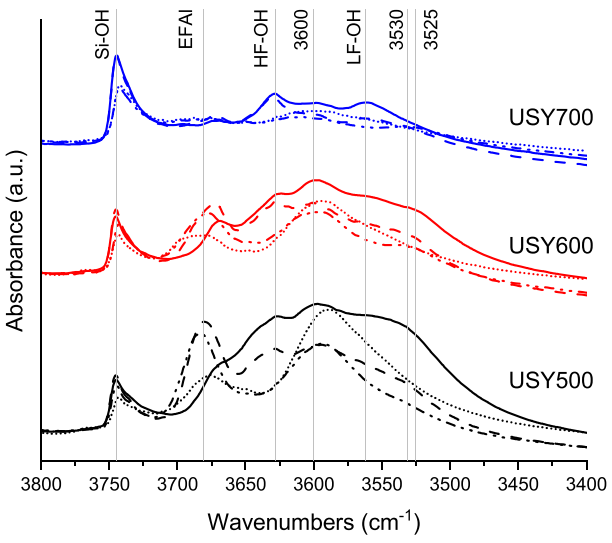

a)

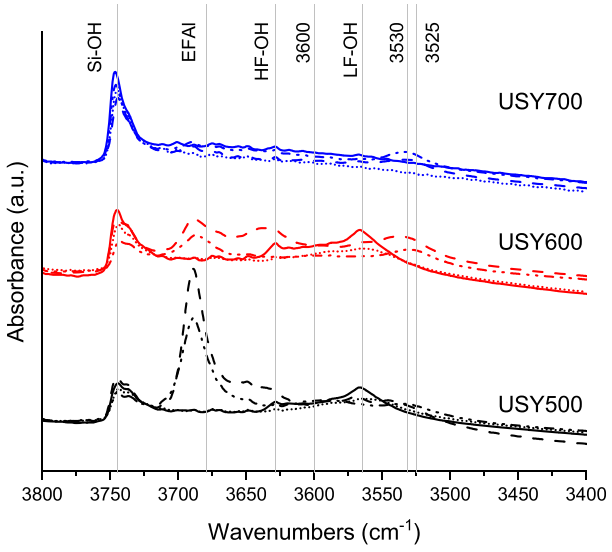

b)

Fig. 1. FT-IR spectra in the OH stretching region for parent USYs (solid lines) and La-USYS (dashed lines) after pretreatment under vacuum at 400 ºC, and for parent USYs (dotted lines) and La-USYs (dash-dotted lines) after pyridine adsorption at 250 ºC. (a) Fresh zeolites; (b) steamed zeolites.

Finally, the ion exchange process seems to slightly reduce the total Al content, as indicated by a small increase of the bulk Si/Al ratio. Probably some of the EFAl species in charge compensation sites have been substituted by cationic La species during the ion-exchange step.

The acidic properties of the fresh high REO-USYs are compared with those of the parent USYs in Table 3 and Table S3. Lanthanum incorporation results in an important decrease of both, the total BAS and the stronger BAS, retaining pyridine at the highest desorption temperature of 400 ºC, but also in a decrease of the LAS density as compared to the La-free USYs.

The FT-IR spectra in the OH stretching region of the IR spectrum can give more information regarding the type and location of the cationic aluminum and lanthanum species present in the samples obtained by means of the different pre-stabilization steps. Fig. 1a shows the spectra corresponding to the parent USYs and the La-USYs (fresh) after pretreatment under vacuum at 400 ºC and after interaction with pyridine and desorption at 250 ºC (solid and dotted lines, respectively).

The three La free zeolites present a complex profile, with the typical bands described for ultrastable Y zeolites [32]. Thus, bands at 3630 and ~3560 cm^{-1}, corresponding to the high frequency (HF) and low frequency (LF) bridged hydroxyls of acidic nature, additional bands at 3600 cm^{-1} and in the range of 3670–3680 cm^{-1}, attributed to the presence of non-acidic extraframework Al species, and the band at 3745 cm^{-1} related to external silanol groups are observed . Samples USY500 and USY600 also present two bands at 3600–3610 and 3525 cm^{-1} assigned to Brønsted acid sites of enhanced strength, resulting from the interaction of the HF and LF hydroxyls with EFAl species [11]. The intensity of all bands decreases when increasing the pre-stabilization temperature, including those related to extraframework aluminum, probably because of the formation of more agglomerated species with no Lewis acid character, [12] in good agreement with the decrease of the Lewis acidity observed, and shown in Table 3. Lanthanum incorporation to USY500 and USY600 (dashed lines in Fig. 1a) results in an increased intensity of the band at ~3680 cm^{-1} corresponding to non-acidic pseudobohemite type EFAl, [35] whereas the one at 3600 cm^{-1} decreases suggesting the possible interaction of La with these EFAl species. An additional band at 3530 cm^{-1}, assigned to non-acidic $LaOH^{2+}$ and $La(OH)_2^+$ species, is also observed. Regarding the acid bridging Al-OH, the intensity of both HF- and LF-OH bands is reduced after La incorporation, although the second one seems to be decreased in a larger extent. This would confirm the preferential location of the cationic La species within the sodalite cages. However, and probably due to the high RE content of these samples, part of it is also compensating charge within the supercages, further decreasing the total BAS density as shown in Table 3.

Hydrothermal treatment of the La-free USYs leads to an important decrease of the acid HF (3630 cm-1) and LF (~3560 cm^{-1}) bridging hydroxyls (see Fig. 1b). Regarding the bands at 3610 and 3525, corresponding to HF- and LF-OH of higher acid strength, the former bands are small, but the latter, related to the –OH pointing into the sodalite cage, are not detected. However, La incorporation has a clear stabilizing effect regarding acidity preservation, as evidenced by the presence of bands at ~3630 and ~3560 cm^{-1}, assigned to the acid bridging hydroxyls corresponding to aluminum in tetrahedral positions within the supercages and within the sodalite cages, which were barely visible after steaming in the absence of RE. Moreover, although the band assigned to HF-Al-OH of enhanced strength (3600–3610 cm^{-1}) is not detected anymore, the LF-Al-OH within the sodalite cage, are still interacting with cationic species, leading to the presence of a second band with acidic nature at lower frequencies (3525 cm^{-1}).

The catalytic behavior of these high REO-USYs (steamed) is compared in Table S4 with that of the steamed parent La-free USYs. In terms of activity, the addition of La makes no significant difference for USY500-ST and USY600-ST. However, it is clearly beneficial in the case of the highly dealuminated USY700-ST, in good agreement with the higher BAS density of La-USY700-ST as compared to USY700-ST. Regarding the selectivity comparison under iso-conversion conditions, in case of the high UC size USY500-based catalysts the introduction of La leads to an increase in dry gas, LPG and coke. The effect of REO addition to USY600 is smaller than for USY500 but, still, a slight decrease in LPG and gasoline is observed, together with a coke increase. Regarding USY700, adding La results in higher LPG and gasoline selectivity and lower coke, although the olefinicity in LPG is slightly reduced.

Thus, what can be concluded from this part of the study is that the physicochemical and acidic properties of the starting USY will play an important role in the incorporation of stabilization elements such as La and in the degree of improvement of its catalytic behavior related to the presence of La.

3.2.2. *Influence of REO content*

According to the results presented in the previous section and in agreement with previous literature on the subject, high REO contents stabilize the USY zeolites as compared to the parent REO-free samples,

Table 4
Physico-chemical properties of La- USY600 with different REO content.

Sample	UCS (Å ± 0.03)	Si/Al_{TOT} (ICP)	Si/Al_{FAL} (UCS)	La_2O_3 (wt%)	BET (m^2/g)	V_{micro} (cm^3/g)	V_{meso} (cm^3/g)	BAS[a] (a.u.)	LAS[a] (a.u.)
USY600-ST	24.35	2.5	10	—	589	0.25	0.12	123	186
0.5La-USY600- ST	24.35	2.7	10	0.5	514	0.20	0.14	85	176
1.2La-USY600- ST	24.32	2.7	12	1.2	517	0.20	0.13	96	189
1.8La-USY600- ST	24.33	2.5	11	1.8	530	0.21	0.13	128	215
4.7La-USY600- ST	24.43	3.1	6	4.7	558	0.23	0.12	99	107

[a] BAS and LAS determined by FT-IR combined with pydirine adsorption and desorption at 250 °C.

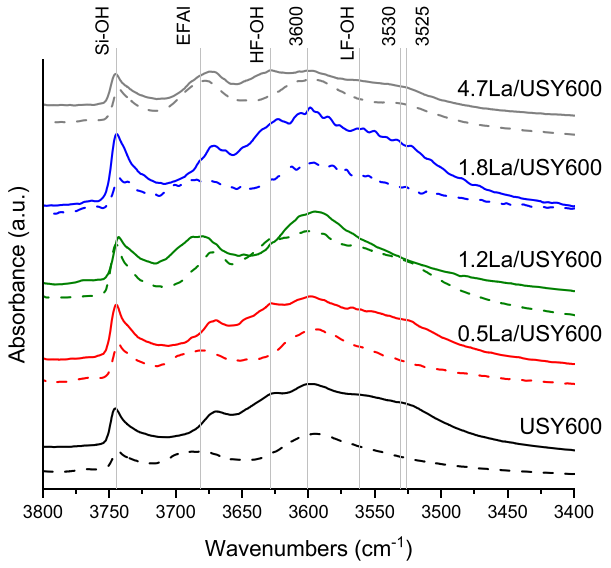

a)

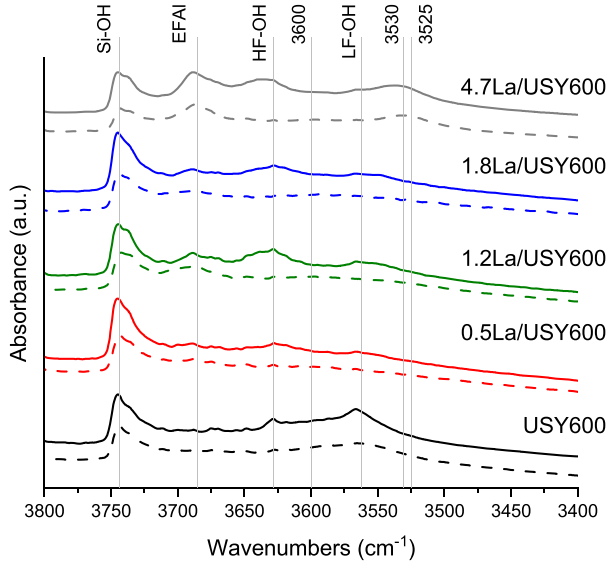

b)

Fig. 2. FT-IR spectra in the OH stretching region for La-USY600 after pre-treatment under vacuum at 400 °C (solid lines), and for parent USYs after pyridine adsorption at 250 °C (dotted lines). (a) Fresh zeolites; (b) steamed zeolites.

thanks to the location of cationic La species in the sodalite cages [23,30,31]. However, the excess La also compensates part of the framework aluminum of the supercages, leading in this way to a significant decrease in the BAS density, especially in the case of USY500 and USY600. Therefore, the benefits of high La contents in terms of activity and selectivity are only observed for low UCS USY700, obtained by a severe pre-stabilization at 700 °C, highly dealuminated and, in consequence, significantly less active than USY500 and USY600, even after REO stabilization.

Table 5
Activity at C/O= 0.5 and selectivity at 85% bottoms conversion of La-USY600 catalysts with different REO contents.

	USY600-ST	1.2La-USY600-ST	1.8La-USY600-ST	4.7La-USY600-ST
2nd order Activity @ C/O= 0.5	1.8	1.8	2.0	2.0
Gasoline Conversion @ C/O= 0.5, %	66.9	63.7	66.3	66.5
Bottoms Conversion @ C/O= 0.5, %	89.0	87.9	90.1	89.8
H_2, wt%	0.1	0.1	0.1	0.1
Total C_2-, wt%	1.4	1.4	1.1	1.4
LPG, wt%	14.9	15.9	12.1	14.1
Gasoline, wt%	40.4	40.3	41.5	40.1
LCO, wt%	26.4	25.3	27.7	27.1
Bottoms, wt%	15.0	15.0	15.0	15.0
Coke, wt%	1.9	2.0	2.5	2.3
$C_3^=$/Total C_3s, wt/wt	0.8	0.8	0.8	0.8
$iC_4^=/iC_4$, wt/wt	0.2	0.2	0.2	0.2
Total $C_4^=$s/Total C_4s, wt/wt	0.5	0.4	0.4	0.5

Thus, La content was reduced for USY600 aiming to confirm if lower REO amounts could lead to similar structure stabilization levels with a lower acidity loss and, eventually, aiming to improve its catalytic behavior. The samples prepared, their REO contents and their main physicochemical properties are given in Table 4. Regarding structure preservation of the final steamed samples, REO contents below 2 wt% result in lower micropore volumes as compared to the parent USY600-ST indicating a larger crystallinity loss, although mesopore volume and, therefore, accessibility, is slightly increased. Regarding the UC size of the samples, it is only increased for the highest REO loading (UC size=24.43 Å) as compared to the La-free USY600 (UC size=24.35 Å), whereas for lower La contents the values are comparable to those of the parent zeolite. However, the BAS density of the La-USY600-ST increases up to a maximum for the intermediate content of 1.8 wt% La_2O_3 and decreases for the highest REO loading (see Table 4 and Table S5). Sample 1.8La-USY600-ST has not only the largest amount of BAS and LAS, but also the highest specific acidity, determined per micropore surface (see Table S5).

In order to understand this maximum observed in acidity preservation for intermediate La contents, the IR spectra in the OH stretching region have been compared for the fresh and steamed samples. According to the spectra compared in Fig. 2a, the four fresh zeolites with La content below 2 wt% present a complex profile, similar to that of the La-free USY600. As La content increases, the intensity of the bands at 3560 and 3524 cm^{-1}, related to the acid hydroxyls pointing into the sodalite cages, decreases progressively, confirming the preference of the La cations for this location within the small cages. Moreover, at the highest La loading a shoulder appears at 3530 cm^{-1}, assigned to nonacidic for $La(OH)^{2+}$, $La(OH)^{2+}$ species, as mentioned before.

The FT-IR spectra corresponding to the steamed samples (see Fig. 2b)

Table 6
Physico-chemical properties of 1.0 P/USYT samples (T = 500, 600 and 700 ºC), steamed at 750 ºC, 5 h (ST).

Sample	UCS (Å)	Si/Al_{TOT} (ICP)	Si/Al_{FAL} (UCS)	P (wt%)	BET (m^2/g)	V_{micro} (cm^3/g)	V_{meso} (cm^3/g)	BAS[a] (a.u.)	LAS[a] (a.u.)
USY500 +ST	24.34	2,5	10	—	585	0.26	0,09	101	168
1.0 P/USY500C-ST	24.27	2.6	20	1.1	430	0.174	0.08	62	115
1.0MAP/USY500C-ST	24.32	3.1	12	1.0	498	0.21	0.07	158	281
1.0DAP/USY500C-ST	24.30	2.7	14	1.0	517	0.23	0.08	71	115
USY600 +ST	24.35	2.5	10	—	589	0.25	0.12	123	186
1.0 P/USY600C-ST	24.30	2.5	14	1.0	437	0.18	0.11	83	138
1.0MAP/USY600C-ST	24.34	2.7	10	1.0	495	0.21	0.10	132	243
1.0DAP/USY600C-ST	24.29	2.8	16	1.1	502	0.21	0.16	53	86
USY700 +ST	24.26	2.5	23	—	466	0.14	0.18	42	76
1.0 P/USY700C-ST	24.24	2.5	33	0.9	425	0.15	0.15	58	104
1.0MAP/USY700C-ST	24.32	2.6	12	1.0	353	0.11	0.12	63	104
1.0DAP/USY700C-ST	24.21	2.6	87	1.1	268	0.09	0.13	21	32

[a] BAS and LAS determined by FT-IR combined with pydirine adsorption and desorption at 250 ºC.

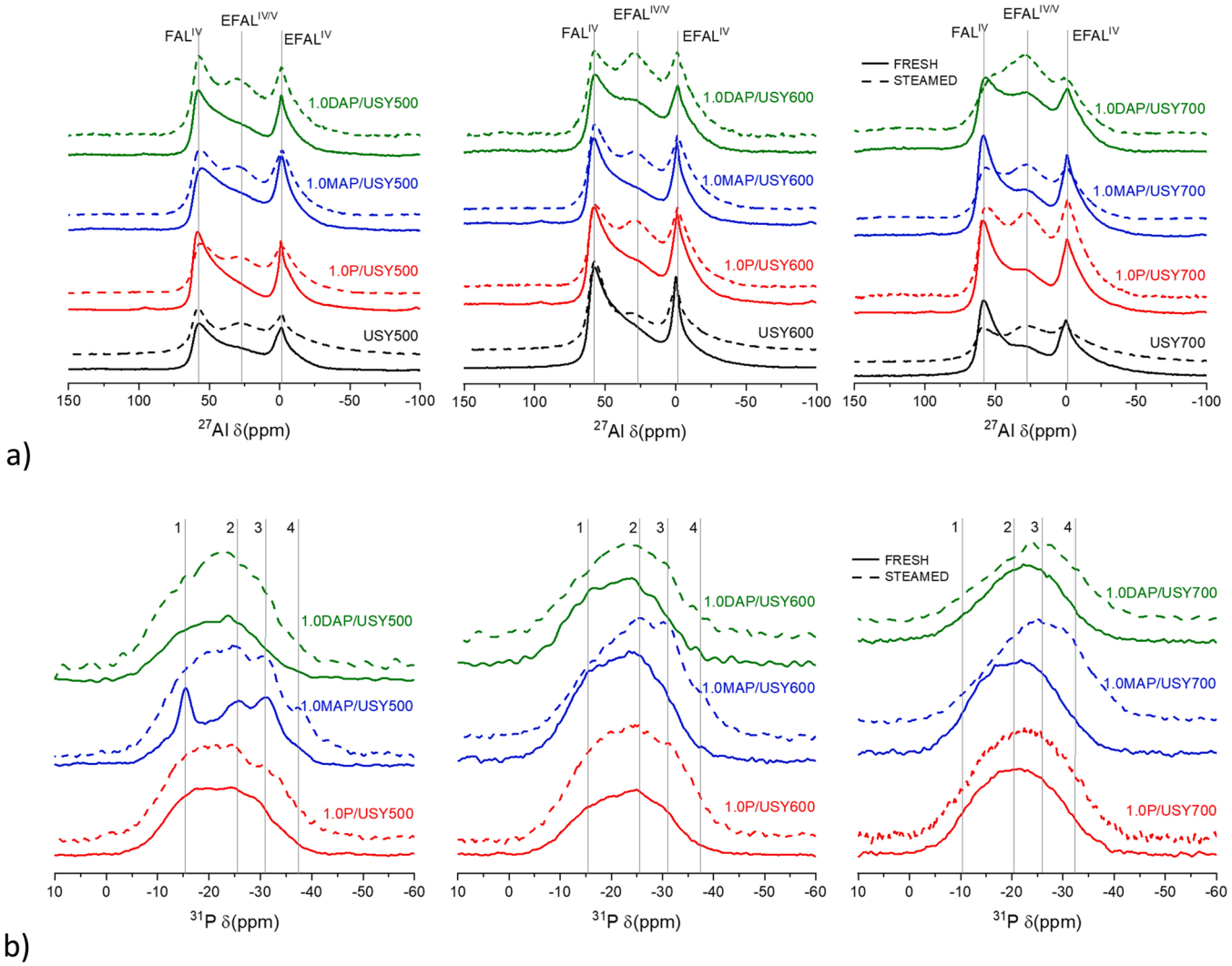

Fig. 3. (a) ^{27}Al- MAS NMR and (b) ^{31}P-MAS NMR spectra of the fresh (continuous lines) and of the steamed (dotted lines) P containing USY's. 1.0 wt% P content added by impregnation with H_3PO_4 as P source. Assignment of P species in (b): 1) Dispersed polyphosphates; 2) amorphous AlPO4; 3) tridymite; 4) Condensed polyphosphates.

clearly show how the bands assigned to HF and LF-OH (3630 and 3560 cm^{-1}, respectively) increase when increasing the REO loading up to 1.8 wt%. However, increasing the amount of La_2O_3 from 1.8 to 4.7 wt % does not further increase the intensity of the HF- and LF-OH bands to a significant extend, whereas a clear increase of the band at 3530 cm^{-1} is observed for the highest REO loading. This band, corresponding to the cationic hydroxylated lanthanum species, will be compensating the charge of FAl and will be, therefore, reducing the number of BAS. Finally, the band appearing at 3690 cm^{-1} starts to be visible at La_2O_3 contents as low as 0.5 wt% (sample 0,5La-USY600-ST) and becomes more intense as the REO amount is increased, evidencing that the presence of this band is directly related to the presence of lanthanum.

Table 7
Activity at C/O= 0.5 and selectivity at 85% bottoms conversion of 1.0 wt% P loaded USY500, USY600 and USY700 catalysts prepared using H_3PO_4.

	1.0 P/ USY500-ST	1.0 P/ USY600-ST	1.0 P/ USY700-ST
2nd order Activity @ C/O= 0.5	1.9	1.5	1.5
Gasoline Conversion @ C/O= 0.5, %	66.0	60.7	59.3
Bottoms Conversion @ C/O= 0.5, %	89.5	85.7	86.1
H_2, wt%	0.1	0.1	0.1
Total C_{2-}, wt%	1.3	1.4	1.2
LPG, wt%	14.1	15.1	14.8
Gasoline, wt%	40.2	41.8	39.0
LCO, wt%	27.0	25.2	27.3
Bottoms, wt%	15.0	15.0	15.0
Coke, wt%	2.4	1.4	2.6
$C_3^=$/Total C_3s, wt/wt	0.8	0.8	0.8
$iC_4^=$/iC_4, wt/wt	0.3	0.3	0.4
Total $C_4^=$s/Total C_4s, wt/wt	0.5	0.5	0.5

Some of the La-USY600 samples (wt% REO=1.2, 1.8 and 4.7) have been tested, after hydrothermal stabilization at 750 ºC for 5 h, as catalysts for VGO cracking in a MAT unit. The results, enclosed in Table 5, show that low REO contents (1.2 wt%) do not improve the activity nor the selectivity as compared to the La-free USY600-ST. Increasing REO to 1.8 wt% or higher slightly improves bottoms conversion without significantly penalizing gasoline conversion. However, intermediate REO contents (1.8 wt%), which resulted in the highest BAS density and the highest specific Brønsted acidity, result in higher coke selectivity and lower selectivity to light olefins. Thus, the best results are obtained, also in the case of USY600, with a low dealumination degree and high structural preservation, for high REO levels.

3.2.3. *P-stabilized USY zeolites*

Phosphorus stabilization of zeolites, mainly ZSM-5, has been extensively studied in the open literature along the last 30 years [46]. Thorough studies on P stabilization of Y and USY zeolites are, however, scarce. Although claimed in the patent literature, [36–41] only a few academic investigations have been published, as far as we know, [34,35] describing the influence of P loading on the thermal and hydrothermal stability of Y-based materials and on their activity and selectivity for catalytic cracking. Corma et al. showed that H_3PO_4 treatments dealuminated the USY framework and led to the formation of amorphous $AlPO_4$-Al_2O_3 phases and even tridymite-type crystalline $AlPO_4$, depending on the thermal and/or hydrothermal conditions applied [35]. Moreover, 1 wt% P was claimed as the optimum P loading in terms of textural and acidic properties preservation [36]. The 1 wt% P containing USYs were also the best performing when tested as catalysts for VGO cracking, when comparing P-USYs with phosphorus loadings in the range of 0.5–6 wt%. Therefore, the study on the influence of the starting USY and of the P source on the hydrothermal stability and the catalytic behavior for cracking of VGO has been done for 1 wt% P containing USY samples and steaming at 750 ºC/5 h.

In a first approach, samples USY500, USY600 and USY700 were impregnated with 1.0 wt% P using H_3PO_4 as the P source and further calcined and steam treated at 750 ºC, for 5 h in a 100% steam atmosphere. The results enclosed in Table 6 show that the stabilization effect of P incorporated by means of the different precursors depends on the properties of the starting USY.

Thus, when using H_3PO_4, the dealumination degree according to the unit cell size, and the crystallinity loss, evidenced by the micropore volume decrease, is higher for high UC size USYs (USY500 and USY600), obtained under milder pre-stabilization conditions, than for CBV700. On the other hand, when USY500 and USY600, less dealuminated and containing more dispersed EFAl species, are impregnated with ammonium phosphate (MAP) or diammonium phosphate (DAP) as the P source, the degree of structure preservation is higher than when employing phosphoric acid, whereas MAP and DAP are less effective for stabilization of USY700.

In good agreement with the differences observed in the physico-chemical properties of the P- loaded USYs when employing different P sources, acidity is also affected. Thus, P incorporation as H_3PO_4 to USY500 and USY600 leads to a considerable decrease of the BAS density as compared to the steamed P-free USYs (see Table 6 and Table S6). However, when H_3PO_4 is used as the P source for USY700, the larger structural stabilization of 1.0P/USY700C-S750 as compared to USY-700-ST results also in a higher number of total and strong BAS. Treatment with MAP of USY500 and USY600 (although in a lower extend for the latter) improves BAS preservation as compared to the corresponding P-free zeolites. Thus, for these samples, addition of 1.0 wt% P as MAP has a true stabilization effect of the zeolites towards the hydrothermal treatment employed here. In the case of the more severely dealuminated USY700 the total Brønsted acidity of the sample treated with H_3PO_4 is slightly lower than that of the sample prepared with MAP (see Table 6). However, the amount of sites able to retain pyridine at 350 and 400 ºC are higher for the former (see Table S6), indicating a larger proportion of sites with medium to strong acidity. Regarding the USYs treated with DAP, the amount of both BAS and LAS is significantly lower as compared to the samples prepared with MAP and H_3PO_4 in the case of USY600 and USY700 based samples, and also lower as compared to the USYs containing no phosphorus.

What can be concluded from this complete study of P stabilization of

Table 8
Physico-chemical properties of La-P/USY500 samples.

Sample	UCS (Å ± 0.03)	Si/Al_{TOT} (ICP)	Si/Al_{FAL} (UCS)	La_2O_3 (wt %)	P (wt %)	BET (m^2/g)	V_{micro} (cm^3/g)	V_{meso} (cm^3/g)	BAS[a] (a.u.)	LAS[a] (a.u.)
USY500-ST	24.34	2.5	10	—	—	586	0.26	0.09	101	168
3.3La/USY500-ST	24.49	2.5	5	3.6	—	595	0.25	0.07	113	112
0.5 P/USY500-ST	24.24	2,6	33	—	0.5	522	0.212	0.102	73	163
1.0 P/USY500-ST	24.27	2,6	20	—	1.2	430	0.174	0.079	62	115
2.0 P/USY500-ST	24.26	2,6	23	—	1.8	301	0.126	0.051	21	40
3.0 P/USY500-ST	24.27	2.5	20	—	2.8	160	0.067	0.028	n.d.[b]	n.d.
La-0.5 P/USY500-ST	24.37	2.8	8	2.3	0.5	454	0.186	0.084	63	75
La-1.0 P/USY500-ST	24.37	2.8	8	2.4	0.9	382	0.161	0.065	51	71
La-2.0 P/USY500-ST	24.41	2.7	7	1.8	1.6	312	0.139	0.035	54	61
La-3.0 P/USY500-ST	24.38	2.7	8	1.1	2.6	123	0.053	0.019	35	37

[a] BAS and LAS determined by FT-IR combined with pydirine adsorption and desorption at 250 ºC.
[b] n.d.: not determined

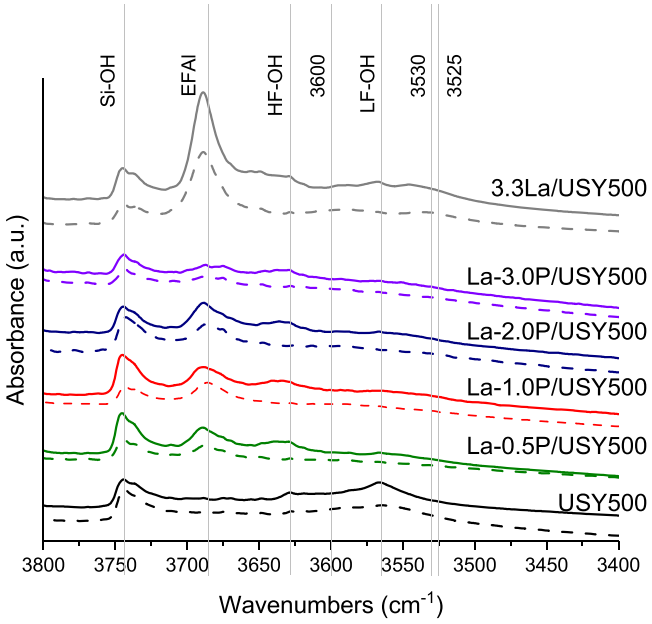

Fig. 4. FT-IR spectra in the OH stretching region for zeolites La-P/USY500-ST. Samples pretreated under vacuum at 400 ºC (solid lines) and after pyridine adsorption at 250 ºC (dotted lines).

USY zeolites is that the stabilization effect in terms of structure and acidity preservation strongly depends on the catalyst preparation conditions and on the properties of the starting USY zeolite. Thus, from the characterization point of view, MAP and DAP are the optimal P sources to stabilize high UCS USYs (USY500 or USY600), but when the starting USY presents a deeper dealumination degree, with highly agglomerated EFAL species (USY700), H_3PO_4 is the best option.

^{27}Al MAS NMR and ^{31}P-MAS NMR of the parent and the 1 wt% P containing USYs, fresh and steamed, were performed in order to study the interaction of P with framework and extra-framework Al (see Fig. 3) on the different samples. ^{27}Al MAS NMR spectrum of the parent USY500 presents the bands corresponding to FAL^{IV} and to EFAL^{VI}, at chemical shifts of 56–58 and − 3–4 ppm respectively, and a third signal assigned to EFAL$^{IV/V}$ at 30 ppm (see Fig. 3a). When impregnating with H_3PO_4 (1 wt%P) and calcining, the proportion of the band at 30 ppm seems to be reduced. This could be due to a possible interaction of P with the amorphous extraframework species. However, and probably due to the relatively low P content (1 wt%) no signals corresponding to tetrahedrally and octahedrally coordinated EFAL in amorphous $AlPO_4$-Al_2O_3 are detected, signals that should appear at 44 and − 6 ppm for the fresh samples and at lower values, around 37 ppm, after steaming.

The bands observed for the P loaded USY600 and 700, prepared with phosphoric acid, are the same as for 1.0P/USY500, but as the pre-stabilization temperature increases from 500 to 700 ºC, the one corresponding to the EFAL$^{IV/V}$ species, at 30 ppm, increases. Regarding the influence of the P source, when moving from H_3PO_4 to MAP and DAP, the proportion of tetrahedrally coordinated FAl increases for the USY500-based samples, both fresh and steamed, but decreases for the P-loaded USY600 and USY700, especially for the latter, where the main band observed is the one assigned to EFAL$^{IV/V}$.

Regarding the ^{31}P-MAS NMR spectra of the fresh samples (Fig. 3b, continuous lines), there are no clearly defined bands. Amorphous $AlPO_4$ gives one broad signal at ~26 ppm, and the proportion of this band is clearly higher for the USY500 and USY600-based samples than for the P-loaded USY700. The two former also present a shoulder at − 30, more intense after steaming (dotted lines), which is assigned to crystalline $AlPO_4$ phases (tridymite). [35] Thus, there seems to be a stronger interaction of P with the less dealuminated USY500 and USY600. On the other hand, there are important differences when comparing the ^{31}P NMR spectra of the samples impregnated with H_3PO_4 with those obtained by treating with MAP and DAP, especially when we focus on the USY500 based samples. When the orthophosphoric acid is used, the main contribution can be assigned to amorphous $AlPO_4$ (−26 ppm). However, this contribution is lower when the preparation is done with MAP, and this makes the signals assigned to dispersed polyphosphates (−15 ppm) and crystalline $AlPO_4$ (−30) clearly visible. When looking at the steamed samples (dotted lines) the signal at − 30 ppm, corresponding to crystalline $AlPO_4$ is more defined for samples 1.0MAP/USY500 and 1.0MAP/USY600 than for the corresponding USYs treated with H_3PO_4 or DAP. The band at − 37 ppm, ascribed to highly condensed polyphosphates, is also more visible for the 1.0MAP series, indicating a lower degree of interaction of the P species with EFAl when added as MAP on these high FAL USYs, than for the H_3PO_4 impregnated samples. Although a single broad band is observed for the USY700 based sample, its maximum is shifted towards more negative chemical shifts for sample 1.0MAP/USY700-S750, and this could be due to a larger contribution of crystalline AlPO4 species. When DAP is the P source amorphous $AlPO_4$ seems to predominate for both, fresh and steamed samples, in all cases.

The different hydrothermal stabilization observed depending on the dealumination degree of the starting USY and on the P source will have a direct influence on the catalytic properties of the P/USYs compared in this section (see Table 7 and Tables S7 to S9 in the SI). Contrary to what might be expected, the activity of the P containing USYs does not correlate with their BAS density or with their textural properties. For the steamed USY500 series, the most active catalyst is the one obtained by impregnation with H_3PO_4, despite its lower acidity, BET, micro- and mesopore surface areas as compared to the steamed parent USY500 or the other two P-loaded USY500 (see Table S7). However, the selectivity to LPG and gasoline is maximum for sample 1.0MAP/USY500-ST, which presents the highest total BAS density. This catalyst is also less selective to coke and to olefins within the LPG fraction as could be expected from a lower dealumination degree and a larger amount of BAS (higher hydrogen transfer capacity). The highest coke selectivity is observed when the sample is prepared using DAP.

The differences in activity are smaller for the USY600 based catalysts (see Table S8), with 1.0P/DAP-USY600-ST being the most active, closely followed by the sample prepared with H_3PO_4, and both outperforming catalyst 1.0MAP/USY600-ST with the highest BAS density. The latter presents the lowest olefinicity in LPG and the lowest $iC_4 = /iC_4$ ratio, confirming a higher hydrogen transfer capacity due to its lower dealumination degree (higher UCS) and higher amount of active sites. As for the USY500 samples, the one prepared by impregnation with DAP is the most selective to coke. Finally, addition of 1 wt% P as H_3PO_4 or MAP to USY700 has a positive effect on the catalyst activity for both, gasoline and bottoms conversion (see Table S9), but impregnation with DAP results in a significantly less active sample. In this particular case, the observed low activity can be explained by a high dealumination degree and an important structural degradation (low BET surface area and micropore volume, see Table 6). In fact, the 2nd order activity and bottoms conversion values given for this sample in Table S9 are obtained at a cat-to-oil ratio of 0.65, and the selectivity values enclosed correspond to a bottoms conversion of 64%, and not 85% as for the rest of the samples. As observed for the USY600 series, stabilization of USY700 with 1.0 wt%P added as MAP leads to the lowest olefins in LPG and the lowest $iC_4 = /iC_4$ ratio. Although the differences are smaller than for the USY600 samples, the lower olefinicity correlates with the higher BAS density of the MAP-based USY700.

As compared to the corresponding P-free USYs, the P/USY500 and P/USY600 are less active, in agreement with the decreased UC size (higher dealumination), BET surface area and micropore volume, directly related to their crystallinity. However, the activity of USY700 is improved when P is incorporated as H_3PO_4 or MAP as compared to the P-free sample.

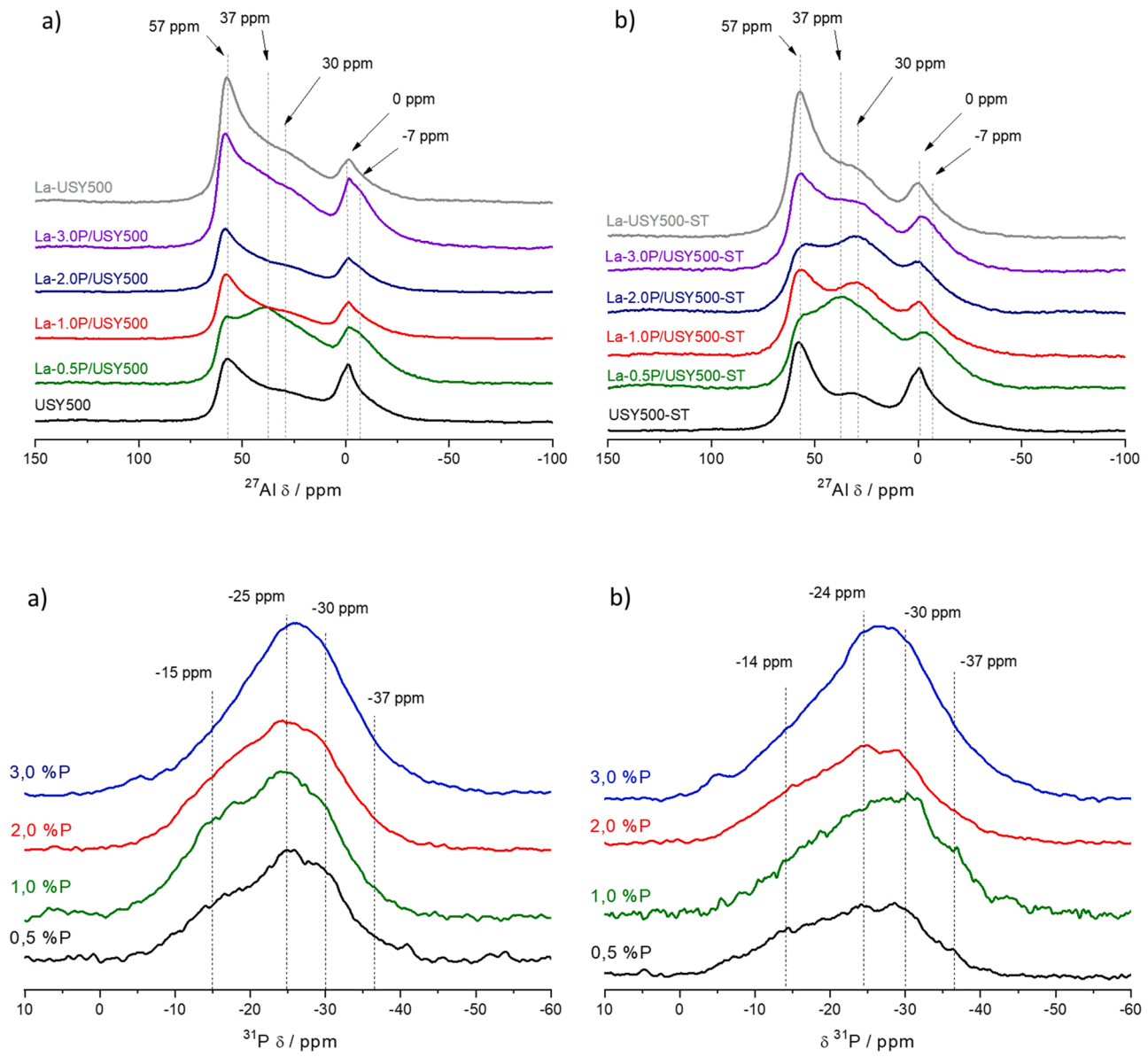

Fig. 5. ^{27}Al-NMR (a, b) and ^{31}P NMR (c, d) spectra of USY500, LaUSY500 and La-P/USY500 with different P contents, fresh (a, c) and after hydrothermal treatment at 750 ºC (b, d).

So far, it has been possible to explain the selectivity of the P/USYs in terms of their BAS density but not their catalytic activity. If we compare the interaction of the three P sources, H_3PO_4, MAP and DAP, with the Al species of the three different USYs after the hydrothermal stabilization (see ^{27}Al and ^{31}P MAS NMR spectra in Fig. 3), it can be seen that impregnation with DAP results in all cases in a decrease of the proportion of tretrahedrally coordinated FAl. This reduction is larger for USY500 and USY700, in agreement with their lower activity. Moreover, the use of MAP leads in all cases to the formation of crystalline $AlPO_4$ and condensed polyphosphates whereas using H_3PO_4 leads to the preferential formation of amorphous $AlPO_4$ by interaction with EFAl species, which plays a beneficial role for the three USYs regarding their catalytic behavior (see Table 7). The effect of this interaction on the total BAS density varies with the degree of dealumination of the zeolite, but in any case it is known to cause the formation new acid sites associated to POH groups, shifting the overall acid site distribution towards milder acidity. [35] This leads to a higher selectivity to liquid fuels and to higher olefin/paraffin ratios in LPG thanks to a reduced recracking and hydrogen transfer capacity.

3.2.4. *La-P/USY500 zeolites*

The study on different P sources described in the former section proved that, in general terms, H_3PO_4 led to the best performing catalysts, irrespective of the prestabilization conditions employed for preparing the USY zeolites (see Table 7). Thus, for the study of the combined La-P stabilization, a set of samples has been prepared by means of impregnation of USY500 with H_3PO_4, to different P loadings in the range of 0.5–3.0 wt% of P, followed by a lanthanum exchange. By adding P in a first step, it will stabilize the zeolite by interacting with the Al species leading to the formation of aluminum phosphate as shown in the former section, reducing and/or avoiding the formation of lanthanum-phosphates after exchange with the RE. The La-P/USY samples have been steamed at 750 ºC for 5 h, in a 100% steam atmosphere and their physicochemical properties are presented in Table 8 and Table S10.

The P contents are close to the target in all cases (see Table 8) whereas the La_2O_3 amount is around 2.3 wt% for the lowest P loadings (0.5–1.0 wt%) and decreases for higher P contents, probably because of the lower ion exchange capacity of these samples.

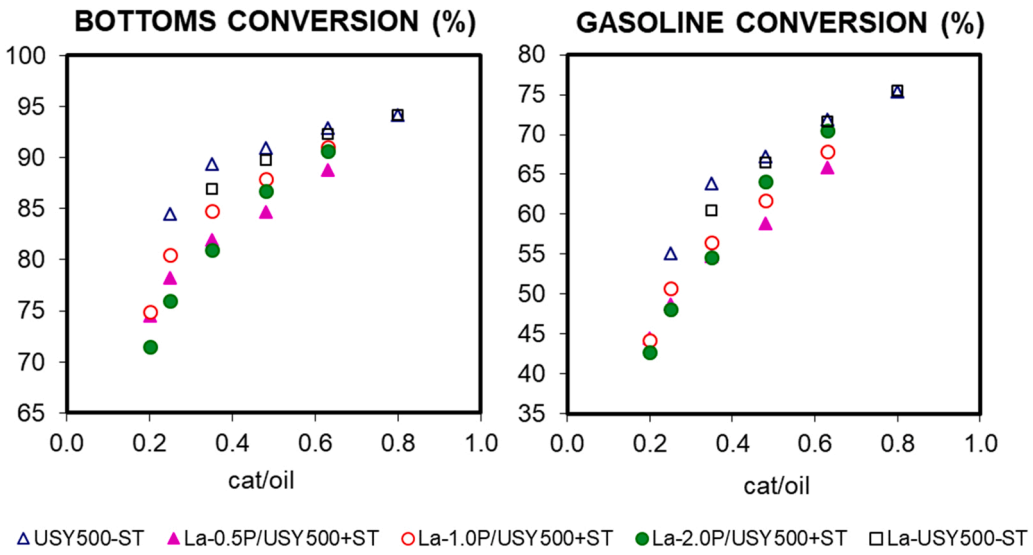

Fig. 6. Gasoline and bottoms conversion obtained with steamed USY500, LaUSY500 and La-P/USY500 with different P contents. VGO cracking in a MAT unit, T = 520 ºC, TOS= 15 s.

The La-P containing samples, steamed at 750 ºC, stabilize at a lower UCS than the LaUSY500-S750, containing no P, and present a lower BET and micropore volume. Still, we have to take into account that the La content in the La-P series is lower, especially for the samples with the highest P content (2–3 wt% P). However, when compared to the P-stabilized USYs, the addition of La as the second stabilization element results in higher UCS values after steaming. As mentioned before, this could be due either to a lower framework dealumination when using the P-La combination or to the increase in the length of the T-O-T bonds induced by the presence of cationic lanthanum. However, BET surface area and micropore volume are reduced as compared to the La-free P-USYs indicating partial crystallinity loss. The sample with 3 wt% P presents a very low BET surface area, probably due to the formation of crystalline $AlPO_4$ phases (tridymite), as will be shown later. In good agreement with a lower dealumination degree, the BAS density of the La-P/USYs is larger preserved as compared to the P/USYs, especially if comparing the samples with the highest P loadings (see Table 8 and Table S10).

Regarding the different Al and La species, according to the FT-IR spectra in the –OH range for the steam treated La-P containing samples compared in Fig. 4, in all cases we can observe the two bands at 3745 and 3680 cm^{-1} assigned to non-acidic hydroxyls, and a broad band centered around 3600 cm-1, also due to EFAl species. As in the case of the La-USYs, an additional band is observed at 3680 cm^{-1}, whose intensity is proportional to the La content. As compared to the parent USY500-ST, the La-P containing zeolites present a single HF-OH band, more intense than that of the La-P-free zeolite, and significantly decreased LF-OH bands. The latter suggests that the P-La combination stabilizes the zeolite in terms of total Brønsted acidity within the large cavities and that, also when incorporated into P-loaded USY500, La moves preferentially into the sodalite cages. The high REO 3.3La/USY500-ST, without P, presents the highest amount of hydroxyls located in the supercages (HF-OH, at 3630 cm^{-1}). This sample also shows a larger contribution of the HF- and LF-OH of enhanced acid strength at 3610 and 3525 cm^{-1}. Thus, the combination of P and La results in intermediate amount of HF-OH acid sites as compared to USY500-ST and 3.3La/USY500-ST, in an important decrease of the LF-OH sites, and in a reduction of the sites with enhanced acid strength.

Figs. 5a and b show the ^{27}Al-MAS NMR spectra of the La-P/USY500 samples, before and after steam treatment at 750 ºC. For the P-free USY500 and La-USY500, the main bands correspond to tetrahedrally coordinated FAl (56–58 ppm), pentacoordinated or distorted tetrahedral EFAl (30 ppm) and octahedrally coordinated EFAl (0 ppm). At low P loadings (La-0.5 P/USY500) two additional bands, at 38 and − 6 ppm assigned to 4- and 6- coordinated aluminum species in amorphous $AlPO_4$-Al_2O_3 [35] are dominating the spectrum, two contributions that decrease significantly as P content increases.

After steam treatment, the proportion of FAl (band at 58 ppm) decreases as compared to the fresh samples, due to an increase of the amount of amorphous $AlPO_4$-Al_2O_3 (~37 ppm) for La-0.5 P/USY500-ST or pentacoordinated or distorted tetrahedral EFAl (30 ppm) in the case of higher P loadings. Moreover, the band assigned to $AlPO_4$-Al_2O_3 shifts to slightly lower resonances, which could be due to the formation of crystalline $AlPO_4$. This would explain the substantial decrease of the BET surface area observed for the sample containing 3.0 wt% P. Fig. 5-b also shows the higher proportion of tetrahedrally coordinated Al present in the LaUSY500-ST sample, which is consistent with its higher UC size value and Brønsted acidity.

The ^{31}P-MAS NMR spectra of the La-P/USY500 samples, before and after steaming at 750 ºC, are compared in Fig. 5c and d, respectively. It is important to note that the band at − 4–5 ppm, attributed to lanthanum phosphate, [47] is not detected in the samples with P loading ≤ 2.0 wt %. However, for sample La-3.0 P/USY500, with the highest P content of 3 wt%, a signal is clearly visible at ~5 ppm, for both the fresh and the steamed zeolite, which could be due to the formation of lanthanum phosphate. On the other hand, the broad signal at − 26 ppm observed in the fresh samples (Fig. 5c) is characteristic of amorphous $AlPO_4$. After steaming at 750 ºC (Fig. 5d) a sharper signal appears at − 30 ppm, which has been assigned to crystalline $AlPO_4$ (tridymite structure). For the two samples with lower P content, fresh, the band at − 15 ppm assigned to the presence of short chain polyphosphates presents a larger contribution. After steam treatment, its intensity decreases and a new resonance appears at − 37 ppm, assigned to highly condensated polyphosphates.

Thus, according to the ^{27}Al- and ^{31}P NMR results the important decreases of BET and micropore volumes at P loadings higher than 1 wt% can be explained by the formation of crystalline $AlPO_4$ phases during the steam deactivation treatment. On the other hand, the characterization results obtained for the La-P/USY samples are in good agreement with results previously published for USY zeolites containing only P [33,35] or La [22,32] indicating that the combination of both stabilizing elements does not lead to the formation of sites different from those described for the single element stabilization.

The catalytic behaviour of the steamed La-P/USYs is compared in Figs. 6 and 7 with that of the reference USY500-ST and La/USY500-ST.

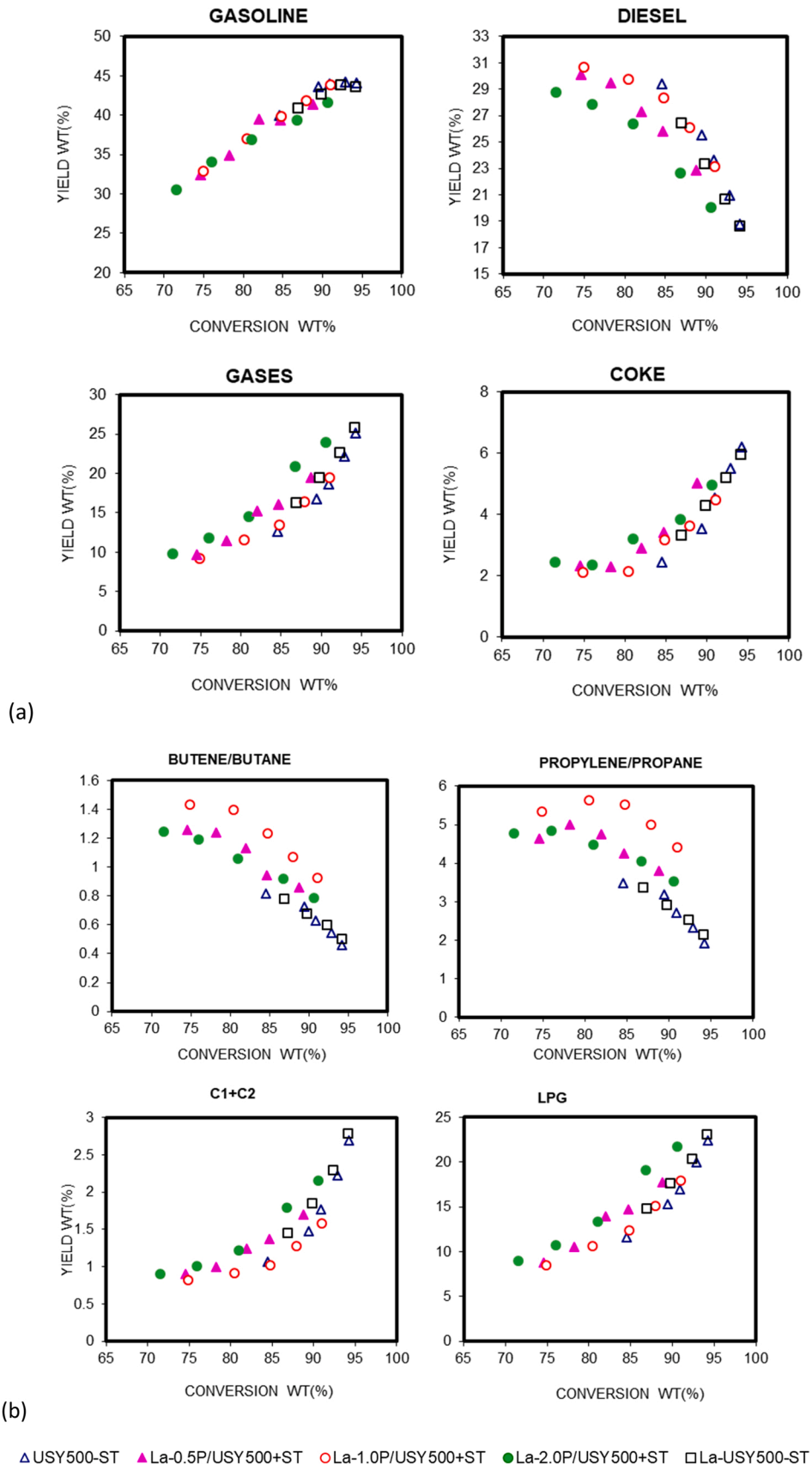

Fig. 7. Selectivity plots comparing steamed USY500, LaUSY500 and La-P/USY500 with different P contents. (a) Overall selectivity, (b) selectivity within the gas fraction. VGO cracking in a MAT unit, T = 520 ºC, TOS= 15 s.

Combined stabilization with P and La results in catalysts with lower activity when compared to P-and La-free and high REO USYs in a MAT unit (see Fig. 6). However, varying the P content it is possible to improve gasoline or bottoms conversion to values closer to those of the P-free La/USY. Thus, lower P contents favour bottoms conversion (87.9% for La-1.0 P/USY500-ST vs 89.8 for La/USY500-ST) whereas intermediate contents result in higher gasoline conversion (64.1% for La-2.0 P/USY500-ST vs 66.5% for La/USY500-ST) when compared at the same cat-to-oil ratio of 0.5. Among the three La-P/USY catalysts and within the range of P contents compared, the sample with 1 wt% P content does not only present a maximum in bottoms conversion, but also in selectivity to gasoline and diesel (see Fig. 7a). This La-P combination also minimizes coke and gases, especially dry gas, and gives overall selectivities comparable to those of the high REO La/USY-ST. Moreover, it presents a significantly higher olefinicity within the LPG fraction at comparable LPG selectivity (see Fig. 7b).

In summary, according to the results presented in Figs. 6 and 7, and in good agreement with the results obtained with the commercial catalysts Phinesse™ and NaphthaMax in the CRU, partial substitution of La by P, leads to comparable hydrothermal stabilization of USY500 as high REO contents. Thus, catalyst La-1.0 P/USY500-ST, a USY zeolite impregnated with 1.0 wt%P in a first step and ion exchanged with La in a second step,although slightly less active than La/USY500-ST, presents comparable overall selectivity and higher selectivity to LPG olefins than the high REO catalyst.

From the former results, we can conclude that the introduction of adequate amounts of P-La, by means of the proper preparation protocol, results in a catalyst with comparable bottoms conversion and overall selectivity as the high REO USY, but with a lower hydrogen transfer capacity, and therefore a higher production of propene and butenes.

4. Conclusions

A rationalized set of USY zeolites has been prepared with different degrees of dealumination and structure preservation. These USYs have been hydrothermally treated after incorporating P, La or a combination of both stabilization elements, in different amounts, and their hydrothermal stability has been studied from the point of view of their physicochemical and catalytic properties. It has been confirmed that the properties of the starting USY zeolite carry a strong influence on the stabilization degree of elements such as P or La. Thus, for USYs obtained under milder pre-stabilization conditions, such as USY500 and USY600, the presence of highly dispersed cationic EFAl species already exerts a stabilization function towards hydrothermal treatments at 750 ºC, and their catalytic behavior is very similar as that of the corresponding high REO La/USY500-ST and La/USY600-ST. Only a strongly dealuminated USY such as USY700, does clearly benefit from the introduction of high REO loadings, thanks to the preservation of a larger amount of BAS. With the aim of avoiding the excess lanthanum to be compensating charge in the supercages of the less dealuminated USYs, the RE loading was reduced. In this way, it was possible to maximize the BAS density for intermediate La contents (1.8 wt%), but the higher amount of active sites did not compensate the crystallinity loss, and the catalytic behavior of the 4.7La/USY600-ST was not improved.

A similar trend was observed when adding P as single stabilization element. Independently of the P source, the activity of the steamed 1.0 P/USY500 and 1.0 P/USY600 was lower than that of the P-free USYs or high REO USYs to both, gasoline and bottoms conversion. Only for the more dealuminated USY700, the addition of 1.0 wt% of P as H_3PO_4 or MAP resulted in a more active catalyst with similar liquid fuels and lower coke selectivity as compared to the reference P-free zeolite and even the La/USY700-ST.

However, the study with the set of USYs prepared has confirmed that it is possible to improve the catalytic behavior of a high UC size USY, with a low dealumination degree, to levels comparable to those given by a high REO La/USY by properly combining P and La as stabilization elements. In good agreement with the industrial field trial observations and with the results obtained in a CRU with the commercial ECATs, a USY zeolite impregnated with 1.0 wt%P in a first step and ion exchanged with La in a second step (catalyst La-1.0 P/USY500-ST) presents comparable overall selectivity and higher selectivity to LPG olefins than the corresponding high REO catalyst.

CRediT authorship contribution statement

All the authors have contributed to the design of experiments, the acquisition and analysis of the experimental data and the writing of the manuscript.

Declaration of Competing Interest

The authors declare that they have no known competing financial interests or personal relationships that could have appeared to influence the work reported in this paper.

Data Availability

No data was used for the research described in the article.

Acknowledgements

This work has been supported by BASF Corporation, by the Spanish Government through PID2021-122755OB-I00 and by the GVA through AICO/2021/201. Financial support by the Spanish Ministry of Science and Innovation (CEX2021-001230-S grant funded by MCIN/AEI/10.13039/501100011033) is gratefully acknowledged. The authors thank Eva Briz for technical assistance and the Electron Microscopy Service of the UPV for their help in sample characterization.

Appendix A. Supporting information

Supplementary data associated with this article can be found in the online version at doi:10.1016/j.cattod.2023.114123.

References

[1] C. Martínez, A. Corma, Inorganic molecular sieves: preparation, modification and industrial application in catalytic processes, Coord. Chem. Rev. 255 (13–14) (2011) 1558–1580, https://doi.org/10.1016/j.ccr.2011.03.014.
[2] W. Vermeiren, J.-P. Gilson, Impact of zeolites on the petroleum and petrochemical industry, Top. Catal. 52 (2009) 31.
[3] E.T.C. Vogt, B.M. Weckhuysen, Fluid catalytic cracking: recent developments on the grand old lady of zeolite catalysis, Chem. Soc. Rev. 44 (20) (2015) 7342–7370, https://doi.org/10.1039/C5CS00376H.
[4] A. Corma, E. Corresa, Y. Mathieu, L. Sauvanaud, S. Al-Bogami, M.S. Al-Ghrami, A. Bourane, Crude oil to chemicals: light olefins from crude oil, Catal. Sci. Technol. 7 (1) (2017) 12–46, https://doi.org/10.1039/C6CY01886F.
[5] F.A. Agblevor, O. Mante, R. McClung, S.T. Oyama, Co-processing of standard gas oil and biocrude oil to hydrocarbon fuels, Biomass-.-. Bioenergy 45 (2012) 130–137, https://doi.org/10.1016/j.biombioe.2012.05.024.
[6] A. Ochoa, H. Vicente, I. Sierra, J.M. Arandes, P. Castaño, Implications of feeding or cofeeding bio-oil in the fluid catalytic cracker (FCC) in terms of regeneration kinetics and energy balance, Energy 209 (2020), 118467, https://doi.org/10.1016/j.energy.2020.118467.
[7] M.W. Jarvis, J. Olstad, Y. Parent, S. Deutch, K. Iisa, E. Christensen, H. Ben, S. Black, M. Nimlos, K. Magrini, Catalytic upgrading of biomass pyrolysis oxygenates with vacuum gas oil using a davison circulating riser reactor, Energy Fuels 32 (2) (2018) 1733–1743, https://doi.org/10.1021/acs.energyfuels.7b02337.
[8] W. Lutz, Stabilizing effect of non-framework AL on the structure of dealuminated y zeolites under hydrothermal conditions, Cryst. Res. Technol. 25 (8) (1990) 921–926, https://doi.org/10.1002/crat.2170250813.
[9] J. Klinowski, J.M. Thomas, C.A. Fyfe, G.C. Gobbi, Monitoring of structural changes accompanying ultrastabilization of faujasitic zeolite catalysts, Nature 296 (5857) (1982) 533–536, https://doi.org/10.1038/296533a0.
[10] M. Ravi, V.L. Sushkevich, J.A. van Bokhoven, Towards a better understanding of lewis acidic aluminium in zeolites, Nat. Mater. 19 (10) (2020) 1047–1056, https://doi.org/10.1038/S41563-020-0751-3.
[11] A. Corma, V. Fornés, F. Rey, Extraction of extra-framework aluminium in ultrastable Y zeolites by (NH4)2SiF6 treatments, I. Physicochem. Charact. Appl. Catal. 59 (1) (1990) 267–274, https://doi.org/10.1016/S0166-9834(00)82203-4.

[12] R.A. Beyerlein, C. Choi-Feng, J.B. Hall, B.J. Huggins, G.J. Ray, Effect of Steaming on the Defect Structure and Acid Catalysis of Protonated Zeolites, Top. Catal. 4 (1997) 27–42.
[13] A. Corma, From Microporous to Mesoporous Molecular Sieve Materials and Their Use in Catalysis. Chem. Rev, American Chemical Society, 2010, https://doi.org/10.1021/cr960406n.
[14] A. Corma, V. Fornes, F.A. Mocholi, J.B. Monton, F. Rey, Influence of Superacid Sites in USY zeolites on gasoil cracking, Prepr. Symp. 35 (4) (1990) 661–668.
[15] A. Corma, M. Faraldos, A. Martinez, A. Mifsud, Hydrogen Transfer on USY Zeolites during Gas Oil Cracking: Influence of the Adsorption Characteristics of the Zeolite Catalysts, in: J. Catal, 122, American Chemical Society, 1990, pp. 230–239.
[16] Q.L. Wang, G. Giannetto, M. Guisnet, Dealumination of zeolites iii. effect of extra-framework aluminum species on the activity, selectivity, and stability of Y zeolites in n-heptane cracking, J. Catal. 130 (2) (1991) 471–482, https://doi.org/10.1016/0021-9517(91)90129-R.
[17] S.W. Addison, S. Cartlidge, D.A. Harding, G. McElhiney, Role of zeolite non-framework aluminium in catalytic cracking, Appl. Catal. 45 (2) (1988) 307–323, https://doi.org/10.1016/S0166-9834(00)83036-5.
[18] A. Corma, V. Fornés, F.A. Mocholí, J.B. Montón, F. Rey, Influence of superacid sites in ultrastable Y zeolites on gas oil cracking, Fluid Catalytic Cracking II ACS Symposium Series (1991) 2–12, https://doi.org/10.1021/bk-1991-0452.ch002.
[19] M.A. Sanchez-Castillo, R.J. Madon, J.A. Dumesic, Role of rare earth cations in Y zeolite for hydrocarbon cracking, J. Phys. Chem. B 109 (6) (2005) 2164–2175, https://doi.org/10.1021/jp0489875.
[20] A. Akah, Application of rare earths in fluid catalytic cracking: a review, J. Rare Earths 35 (10) (2017) 941–956, https://doi.org/10.1016/S1002-0721(17)60998-0.
[21] A. Corma, V. Fornes, F.V. Melo, J. Herrero, Comparison of the Information given by Ammonia TPD and Pyridine Adsorption-Desorption on the Acidity of Dealuminated HY and LaHY Zeolite Cracking Catalysts, in: Zeolites, 7, American Chemical Society, 1987, pp. 559–563, https://doi.org/10.1016/0144-2449(87)90098-4.
[22] A. Corma, V. Fornes, J.B. Monton, A.V. Orchilles, Structural and Cracking Properties of REHY Zeolites. Activity, Selectivity, and Catalyst-Decay Optimization for n-Heptane Cracking. Ind. Eng. Chem. Prod. Res. Dev, American Chemical Society, 2010, pp. 231–238.
[23] B. Herreros, P.P. Man, J.-M. Manoli, J. Fraissard, Solid-state 139La NMR investigation of lanthanum-exchanged Y zeolites, J. Chem. Soc. Chem. Commun. No. 6 (1992) 464–466, https://doi.org/10.1039/C39920000464.
[24] F. Roessner, K.-H. Steinberg, H.Ir Winkler, n.m.r, 1H longitudinal relaxation studies of the cation distribution in rare-earth and calcium exchanged Y, Zeolites. Zeolites 7 (1) (1987) 47–53, https://doi.org/10.1016/0144-2449(87)90119-9.
[25] L.V.C. Rees, T. Zuyi, Rare-earth ion exchange in zeolite Y, Zeolites 6 (3) (1986) 201–205, https://doi.org/10.1016/0144-2449(86)90048-5.
[26] D. Keir, E.F.T. Lee, L.V.C. Rees, Catalytic activity of differently prepared, fully exchanged lanthanum Y zeolites, Zeolites 8 (3) (1988) 228–231, https://doi.org/10.1016/S0144-2449(88)80312-9.
[27] E.F.T. Lee, L.V.C. Rees, Effect of calcination on location and valency of lanthanum ions in zeolite Y, Zeolites 7 (2) (1987) 143–147, https://doi.org/10.1016/0144-2449(87)90076-5.
[28] E.F.T. Lee, L.V.C. Rees, Dehydroxylation of lanthanum exchanged zeolite Y, Zeolites 7 (6) (1987) 545–548, https://doi.org/10.1016/0144-2449(87)90095-9.
[29] J.W. Roelofsen, H. Mathies, R.L. de Groot, P.C.M. van Woerkom, H.A. Gaur, Effect of Rare Earth Loading in Y-Zeolite on Its Dealumination during Thermal Treatment, in: Y. Murakami, A. Iijima, J.W.B.T.-S. Ward, in S. S., C. (Eds.), New Developments in Zeolite Science and Technology;, Vol. 28, Elsevier, 1986, pp. 337–344, https://doi.org/10.1016/S0167-2991(09)60891-0.
[30] F. Schüßler, E.A. Pidko, R. Kolvenbach, C. Sievers, E.J.M. Hensen, R.A. van Santen, J.A. Lercher, Nature and location of cationic lanthanum species in high alumina containing faujasite type zeolites, J. Phys. Chem. C. 115 (44) (2011) 21763–21776, https://doi.org/10.1021/jp205771e.
[31] J.A. van Bokhoven, A.L. Roest, D.C. Koningsberger, J.T. Miller, G.H. Nachtegaal, A. P.M. Kentgens, Changes in structural and electronic properties of the zeolite framework induced by extraframework Al and La in H-USY and La(x)NaY: A 29Si and 27Al MAS NMR and 27Al MQ MAS NMR Study, J. Phys. Chem. B 104 (2000) 6743.
[32] A. Corma, V. Fornés, J.B. Monton, A.V. Orchilles, Comparison of the activity, selectivity and decay properties of lay and hyultrastable zeolites during the cracking of alkanes, Appl. Catal. 12 (1) (1984) 105–116, https://doi.org/10.1016/S0166-9834(00)81508-0.
[33] T. Blasco, A. Corma, Hydrothermal stabilization of ZSM-5 catalytic-cracking additives by phosphorus addition 237 (2006) 267–277, https://doi.org/10.1016/j.jcat.2005.11.011.
[34] W. Kolodziejski, V. Fornes, A. Corma, Solid-State NMR Study of Ultrastable Zeolite Y Modified with Orthophosphoric Acid, in: Solid State Nucl. Magn. Reson, 2, American Chemical Society, 1993, pp. 121–129.
[35] A. Corma, V. Fornes, W. Kolodziejski, L.J. Martinez-Triguero, Orthophosphoric Acid Interactions with Ultrastable Zeolite Y: Infrared and NMR Studies, in: J. Catal, 145, American Chemical Society, 1994, pp. 27–36.
[36] Corma, A.; Grande-Casas, M.; Martinez-Triguero, J. Process for the Preparation of Catalysts Based on Zeolites Treated with Phosphoric Acid, Useful for Catalytic Cracking Units. WO94/21378, 1994.
[37] G.M. Smith, R. McGuire Jr., B. Yilmaz, Phosphorus-Modif. FCC Catal. (2015).
[38] G.M. Smith, R. McGuire Jr., B. Yilmaz, FCC Catal. Compos. Contain. Boron Oxide Phosphorus (2015).
[39] Q. Fu, C.P. Kelkar, Phosphorus Modif. Crack. Catal. Enhanc. Act. Hydrothermal Stab. (2013).
[40] G.K. Chitnis, J.A. Herbst, Attrition-Resist. Crack. Catal. Contain. Phosphate-Treat. Zeolites (1992).
[41] L.A. Pine, N.L. Cull, Phosphorus-Contain. Catal. Catal. Crack. Process Util. It. EP95364 (1983).
[42] Shackleford, A.; Masak, T.; Fu, Q.; Yilmaz, B.; Culp, R.D.; Gawecki, P. An alternative to rare earth elements in FCC catalysts - the use of Phinesse at Shell Sarnia ⟨www.digitalrefining.com/article/1001234⟩.
[43] J.B. McLean, W.A. Weber, D.H. Harris, Distributed matrix structures – a technology platform for advanced FCC catalytic solutions, NPRA Annu. Meet. (2003) 03–38.
[44] Breton, T. Critical Raw Materials Act: securing the new gas & oil at the heart of our economy ⟨https://ec.europa.eu/commission/presscorner/detail/en/STATEMENT_22_5523⟩ (accessed Nov 30, 2022).
[45] A. Corma, V. Fornés, A. Martínez, A.V. Orchillés, Parameters in Addition to the Unit Cell That Determine the Cracking Activity and Selectivity of Dealuminated HY Zeolites, in: Perspectives in Molecular Sieve Science; ACS Symposium Series, Vol. 368, American Chemical Society, 1988, pp. 35–542, https://doi.org/10.1021/bk-1988-0368.ch035.
[46] H.E. van der Bij, B.M. Weckhuysen, Phosphorus promotion and poisoning in zeolite-based materials: synthesis, characterisation and catalysis, Chem. Soc. Rev. 44 (20) (2015) 7406–7428, https://doi.org/10.1039/C5CS00109A.
[47] L. Dithmer, A.S. Lipton, K. Reitzel, T.E. Warner, D. Lundberg, U.G. Nielsen, Characterization of phosphate sequestration by a lanthanum modified bentonite clay: a solid-state NMR, EXAFS, and PXRD study, Environ. Sci. Technol. 49 (7) (2015) 4559–4566, https://doi.org/10.1021/es506182s.